Scientia Iranica, Vol. 14, No. 4, pp 358–368

SCIENTIA
IRANICA

Research Note

Evaluation of Empirically Derived PVT Properties for Middle East Crude Oils

M.N. Hemmati* **and R. Kharrat**[1]

PVT properties are important parameters in reservoir engineering. Correlations are used whenever experimentally derived PVT data are not available and data from local regions are expected to give better approximation to estimated PVT values. This paper evaluates the most frequently used empirical black oil PVT correlations for application in the Middle East. As will be discussed, Empirical PVT Correlations for Middle East crude oil have been compared as a function of commonly available PVT data. Correlations have been compared for: Bubble point pressure; solution gas oil ratio at bubble point pressure and oil formation volume factor at bubble point pressure. Often, these properties are required for oil field computations when there are no experimental or laboratory measurements available. For comparison of correlations, a wide range of data has been covered. Approximately, five hundred Pressure-Volume-Temperature (PVT) reports have been used in the comparison correlations. The PVT correlations can be ordered with respect to their accuracy: (a) Bubble point pressure: The result of Al-Marhoun and Standing are similar to Hanafy, Dindoruk; (b) Oil formation volume factor: Petrosky, Glaso and Dokla correlations produce similar results, while Al-Marhoun, Standing and Hanafy predictions are different and (c) Solution gas oil ratio: Standing and Al-Marhoun results are the same, however, Dindoruk, Glaso and Petrosky correlations are less accurate. Error bounds of the obtained correlations are calculated and compared to Middle East crude oil. All reservoir fluid property correlations available in the petroleum engineering literature were compared with this database.

INTRODUCTION

The calculation of reserves in an oil reservoir or the determination of its performance and economics requires a good knowledge of the fluids physical properties. Bubble point pressure, GOR and OFVF are of primary importance in material balance calculation. Ideally, these properties are determined from laboratory studies on samples collected from the bottom of the well bore or from the surface. Such experimental data are, however, not always available because of one or more of these reasons: a) Samples collected are not reliable, b) Samples have not been taken because of cost saving, c) PVT analyses are not available when needed. This situation often occurs in production test interpretation wells.

In such cases, PVT properties must be determined by using empirical derived correlations. Obviously, the accuracy of such correlations is critical for the above-mentioned calculations and it is not often known in advance.

Despite the great number of work performed in the past 50 years on PVT correlations, each of them seems to be applicable with a good reliability only in a well-defined range of reservoir fluid characteristics. This is because each correlation has been developed by using samples belonging to a restricted geographical area, with similar fluid compositions and API gravity. In particular, for oil with gravity less than 22°API, the literature is very poor and nearly absent for oil with gravity less than 10°API.

DATA DESCRIPTIONS

More than 50 Middle East oil fields were selected for this study. These fields were selected because, they produce the crude of black oil in nature and the availability of complete PVT reports that are necessary for the evaluation and development of the black oil

*. *Corresponding Author, The Research Center of Petroleum University, Tehran, I.R. Iran.*
1. *The Research Center of Petroleum University, Tehran, I.R. Iran.*

Table 1. Data description for bubble point pressure, GOR, and bubble point oil FVF correlations.

Number of Points	PVT Property	Minimum	Maximum	Mean
499	Bubble point pressure, psia	130	5156	2370.5
499	Solution GOR, SCF/STB	26	2266	715.15
499	FVF, bbl/STB	1.03	2.54	1.41
499	Temperature, °F	74	290	165
499	Stock tank oil gravity, °API	18.80	68.50	31.53
499	Gas gravity (air=1)	0.523	1.50	0.94

Table 2. Range for bubble point pressure, solution GOR and oil FVF correlations.

Properties	Standing [1]	Al-Marhoun [2]	Glaso [3]	Petrosky-Farshad [4]
Tank oil gravity, °API	16.5 to 63.8	19.4 to 44.6	22.3 to 48.1	16.3 to 45
Bubble point pressure, psia	130 to 7000	130 to 3573	165 to 7142	1574 to 6523
Reservoir temperature, °F	100 to 258	74 to 240	80 to 280	114 to 288
Oil FVF at bubble point, bbl/STB	1.024 to 2.15	1.032 to 1.997	1.025 to 2.588	1.1178 to 1.6229
Solution GOR, SCF/STB	20 to 1425	26 to 1602	90 to 2637	217 to 1406
Total surface gas gravity (air=1)	0.59 to 0.95	0.752 to 1.367	0.65 to 1.276	0.5781 to 0.8519
Separator pressure, psia	256 to 465	-	415 (mean)	-
Separator temperature, °F	100 (mean)	-	125 (mean)	-
Reservoir pressure, psia	-	20 to 3573	-	1700 to 10692

correlations. From these oilfields, 499 laboratory PVT analyses were obtained and used to compare the correlations. Descriptions of the data utilized in comparison of each correlation are shown in Table 1 and the range of input data used by each author in developing his correlation is provided in Table 2.

COMPARISON OF CORRELATIONS

Statistical Error Analysis

Average percent relative error, average absolute percent relative error, minimum /maximum absolute percent relative error, standard deviation and correlation coefficient were computed for each correlation.

Bubble Point Pressure

Table 3 shows the statistical error analysis results of the bubble-point pressure correlations. Al-Marhoun's [2] correlation gives low values of Absolute Average Percent Relative Error (AAPRE) and standard deviation of 6.999 percent and 9.26 percent, respectively. A lower value of AAPRE indicates a better accuracy of the correlation. The correlation coefficient of the correlation is almost equal to 1.0(0.977). This shows that a good agreement exists between experimental and calculated bubble point pressure. In comparison with other known correlations, Al-Marhoun's correlation gives lowest AAPRE and standard deviation. This shows that Al-Marhoun's correlation predicts better bubble point pressure for Middle East crude oil than any other known correlations.

The cross plot of the experimental against the calculated bubble point pressure using correlations are presented in Figures 1 through 7. Most of the data points of the Al-Marhoun correlation fall very close to the perfect correlation of a 45° line. A graphical plot of residual (the difference between experimental and calculated bubble point pressure) and experimental bubble point pressure (shown in Figure 1) demonstrated a uniform distribution of errors with most of the data points falling within a ± 500 psia residual line.

Bubble Point Oil FVF

The statistical error analysis results of the bubble point oil FVF correlation are compared in Table 4. The Petrosky correlation [4] gives a better accuracy in estimating bubble point oil FVF for Middle East crude oil. Amongst the correlations, both Petrosky [4] and Glaso [3] correlations seem to be good correlations, their absolute average deviatons and standard deviations are very close and give the lowest values of AAPRE. AAD and standard deviation for Glaso

Table 3. Summary of statistical measures for P_b for common correlations.

Parameters	Petrosky [4]	Glaso [3]	Standing [1]	Al-Marhoun [2]	Dindoruk [5]	Dokla [6]	Hanafy [7]
% AAD	42.33	23.45	10.49	6.999	42.43	17.87	22.64
% ARE	-18.25	20.94	6.185	-4.14	38.54	-0.197	17.83
% Max Dev.	784.5	73.13	70.08	43.66	114.21	197.81	192.34
% Min Dev.	0.013	0.281	0.009	0.021	1.010	0.043	0.111
Std. Dev.	112.75	26.87	14.41	9.26	45.25	26.87	34.69
r	0.882	0.865	0.927	0.977	Minus	0.903	0.930

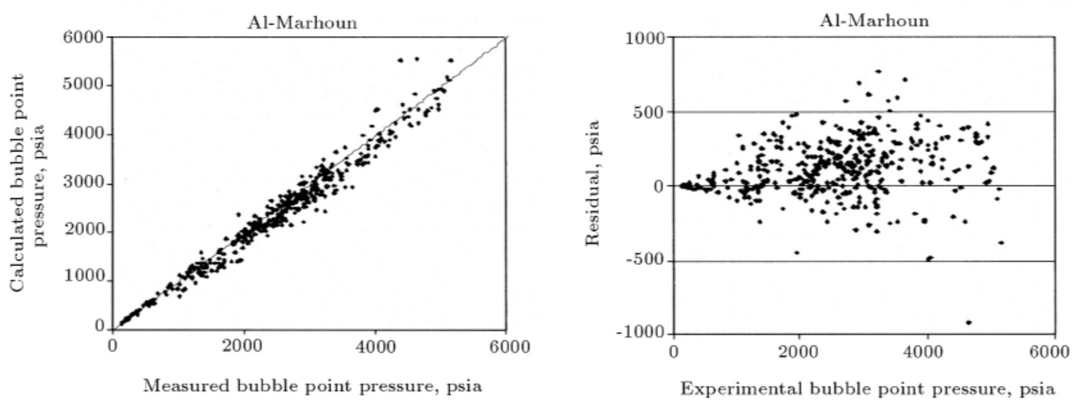

Figure 1. Cross plot and residual plot of P_b (Al-Marhoun [2]) based on Middle East PVT data.

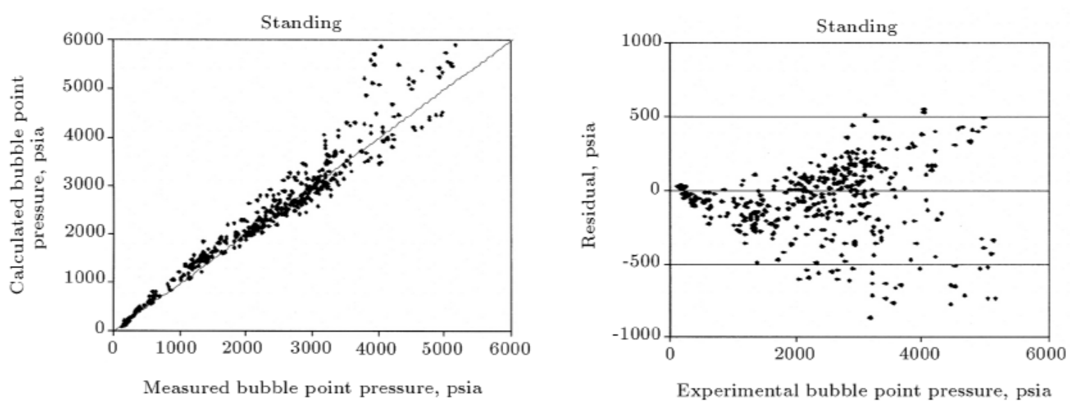

Figure 2. Cross plot and residual plot of P_b (Standing [1]) based on Middle East PVT data.

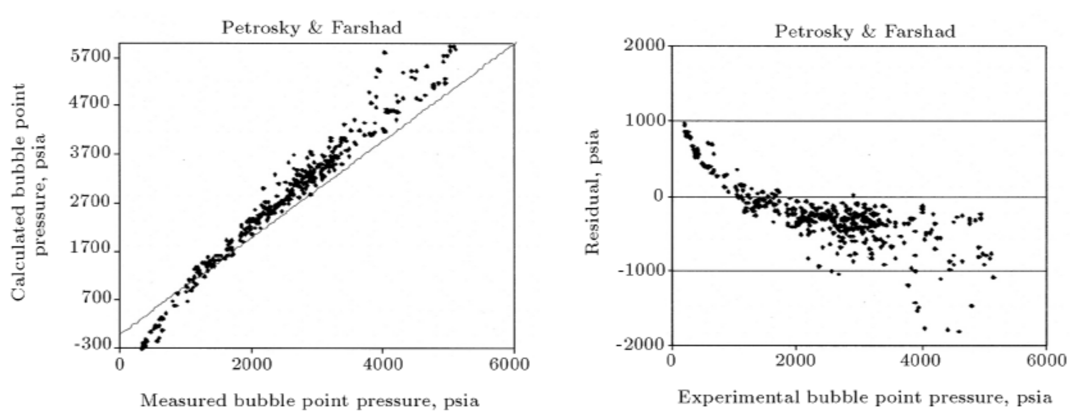

Figure 3. Cross plot and residual plot of P_b (Petrosky [4]) based on Middle East PVT data.

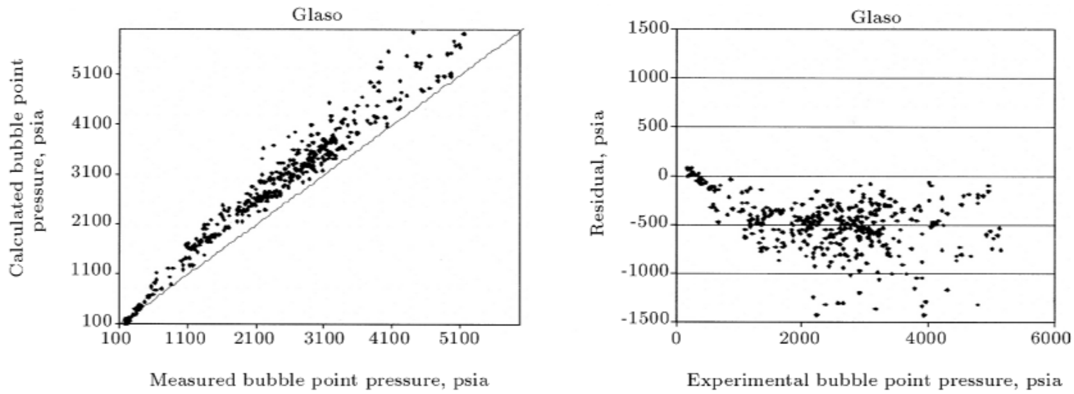

Figure 4. Cross plot and residual plot of P_b (Glaso [3]) based on Middle East PVT data.

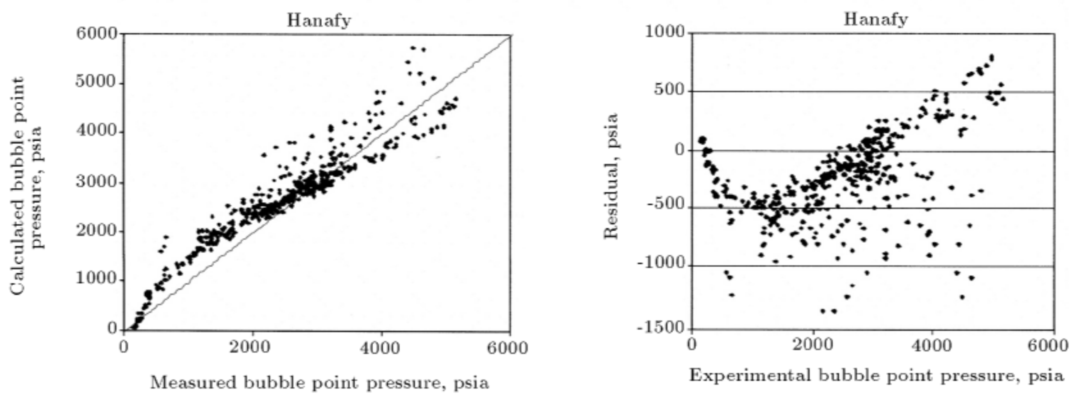

Figure 5. Cross plot and residual plot of P_b (Hanafy [7]) based on Middle East PVT data.

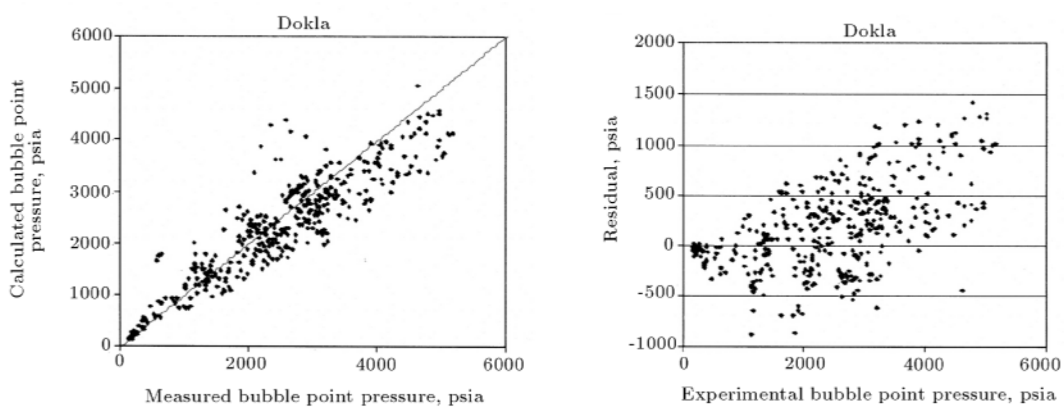

Figure 6. Cross plot and residual plot of P_b (Dokla [6]) based on Middle East PVT data.

Table 4. Summary of statistical measures for B_{ob} for common correlations.

Parameters	Al-Marhoun [2]	Standing [1]	Glaso [3]	Petrosky [4]	Dokla [6]	Dindoruk [5]	Hanafy [7]
% AAD	1.96	1.93	2.157	1.45	2.608	4.39	8.55
% ARE	-1.481	0.98	-0.68	0.26	-1.38	2.60	8.48
% Max Dev.	15.25	11.73	12.28	13.76	13.08	26.94	23.44
% Min Dev.	0.002	0.001	0.006	0.004	0.005	0.009	0.025
Std. Dev.	2.98	2.74	2.84	2.28	3.4	5.61	9.27
r	0.975	0.945	0.984	0.989	0.983	0.945	0.816

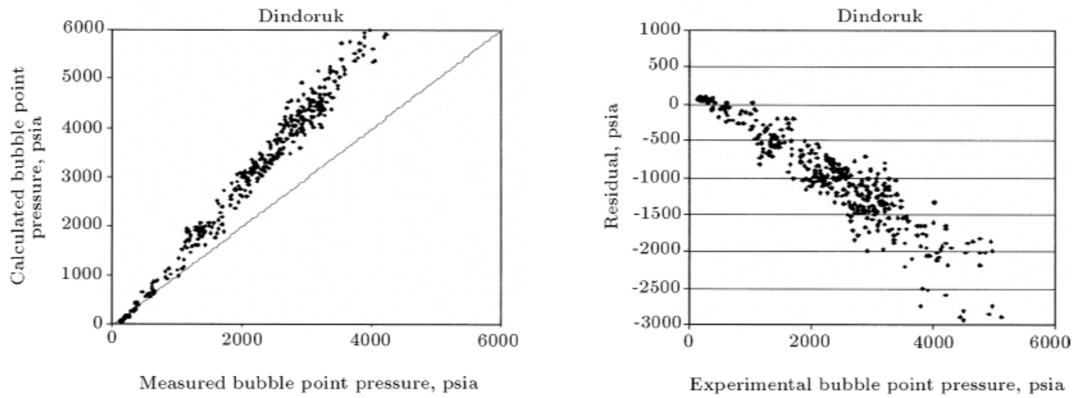

Figure 7. Cross plot and residual plot of P_b (Dindoruk [5]) based on Middle East PVT data.

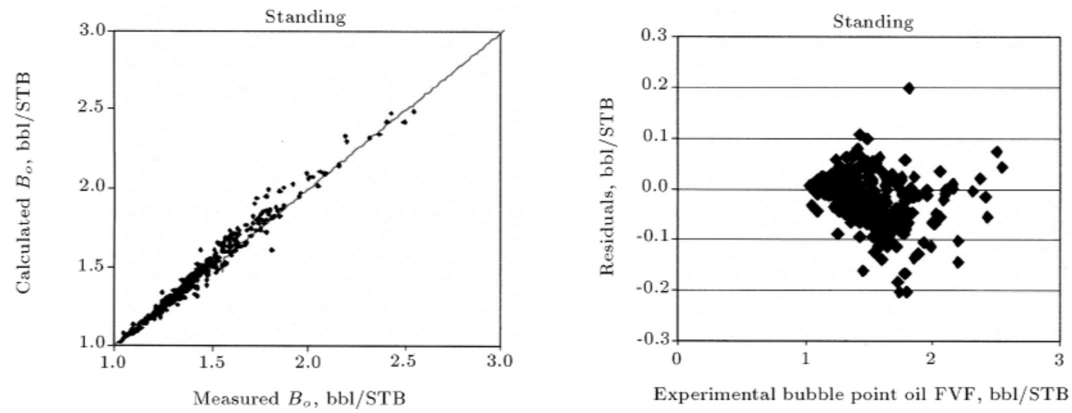

Figure 8. Cross plot and residual plot of B_o (Standing [1]) based on Middle East PVT data.

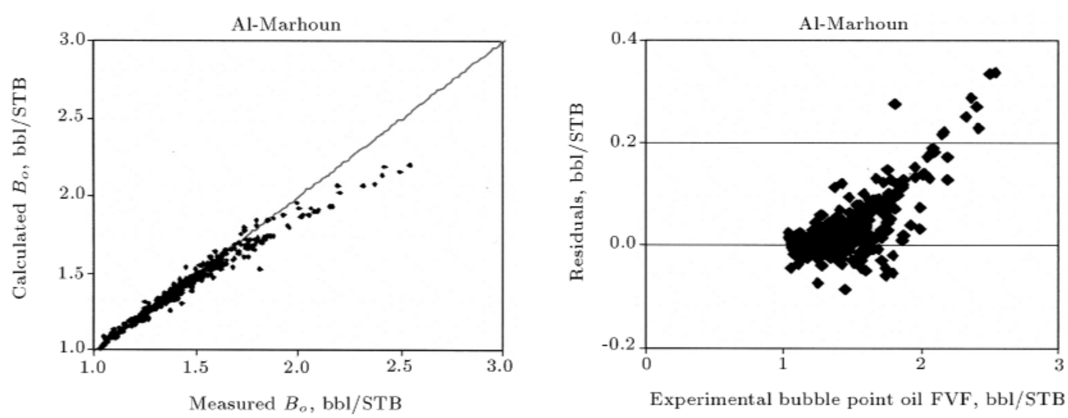

Figure 9. Cross plot and residual plot of B_o (Al-Marhoun [2]) based on Middle East PVT data.

and Petrosky are 2.157 and 1.45 percent, 2.84 and 2.28 percent, respectively. The correlation coefficient is 0.984 and 0.989, respectively, which is close to an ideal value of 1.0. This shows that the Petrosky and Glaso correlations correlate better with experimental data than any other correlations.

The residual plot of the bubble point oil formation volume factor obtained from correlations are shown in Figures 8 through 14. It is clear that the most data points in Figures 10 and 11 lie between $\pm$ 0.2 residual lines. A small residual value indicates a better accuracy of Glaso and Petrosky correlation in estimating the bubble point oil FVF for Middle East crude oil.

Solution GOR

The statistical error analysis results of the Solution GOR correlation are compared in Table 5. It shows

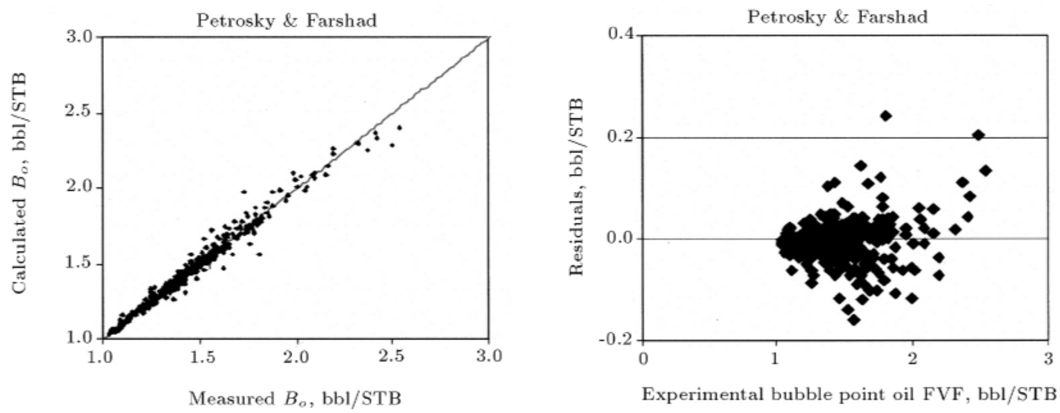

Figure 10. Cross plot and residual plot of B_o (Petrosky [4]) based on Middle East PVT data.

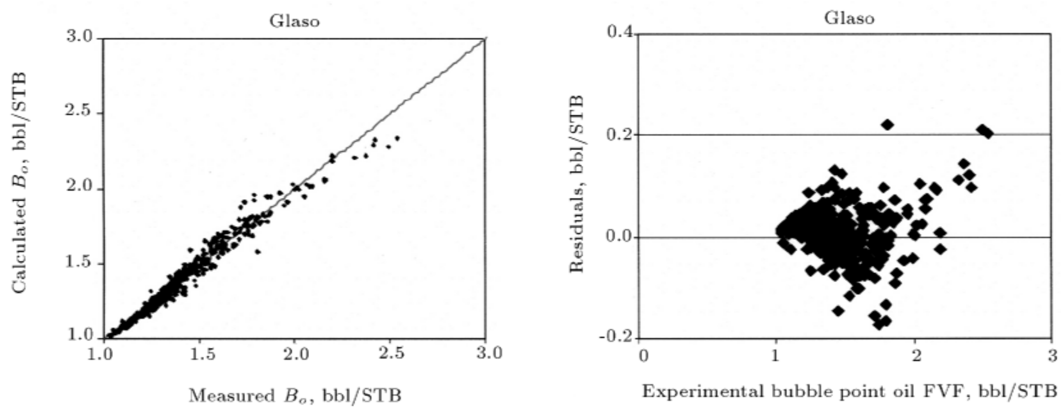

Figure 11. Cross plot and residual plot of B_o (Glaso [3]) based on Middle East PVT data.

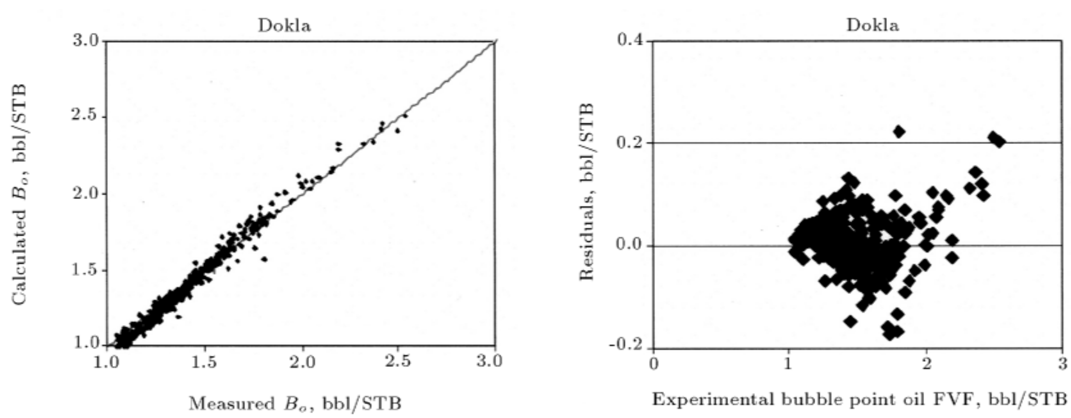

Figure 12. Cross plot and residual plot of B_o (Dokla [6]) based on Middle East PVT data.

Table 5. Summary of statistical measures for solution GOR for common correlations.

Parameters	Al-Marhoun [2]	Standing [1]	Glaso [3]	Petrosky [4]	Dindoruk [5]
%AAD	10.17	9.45	19.84	22.45	17.93
%ARE	7.83	-4.73	-19.55	0.53	3.68
%Max. Dev.	49.45	33.77	40.86	300.63	150.4
%Min. Dev.	0.0295	0.0009	0.248	0.152	0.0138
Std. Dev.	13.58	11.78	21.39	44.84	26.76
r	0.960	0.964	0.890	0.862	0.921

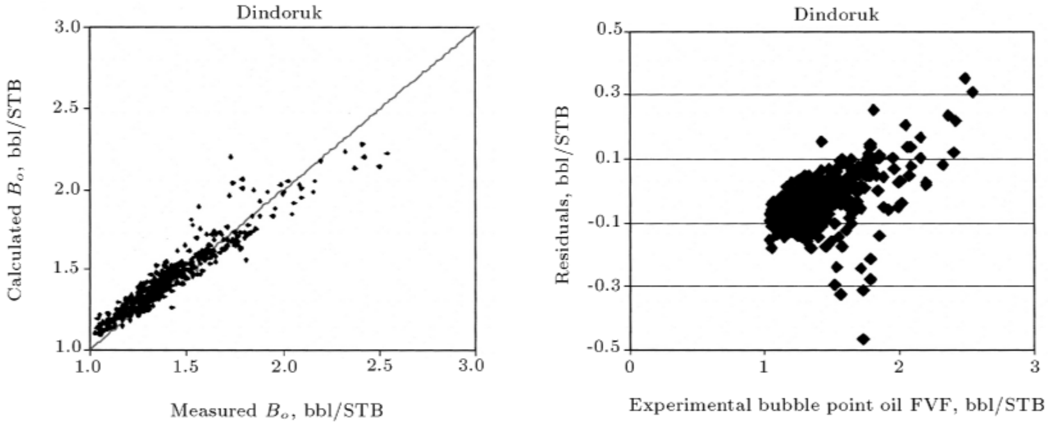

Figure 13. Cross plot and residual plot of B_o (Dindoruk [5]) based on Middle East PVT data.

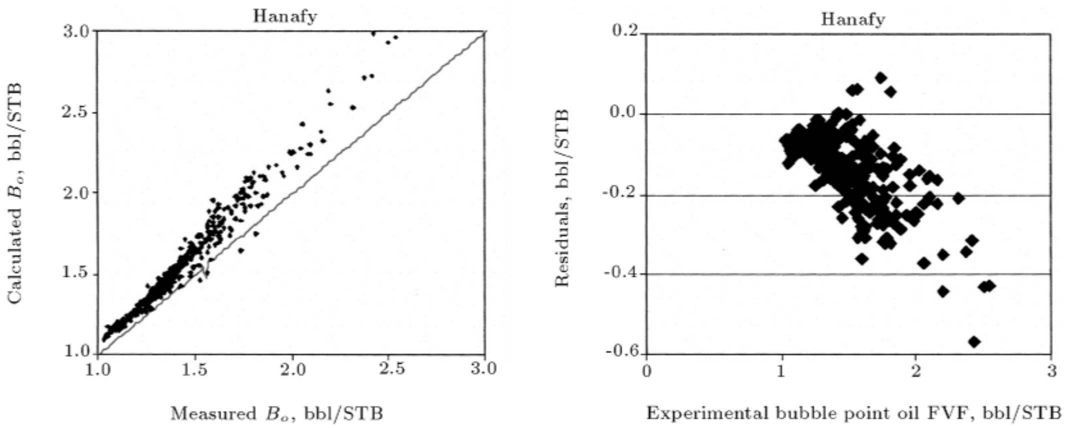

Figure 14. Cross plot and residual plot of B_o (Hanafy [7]) based on Middle East PVT data.

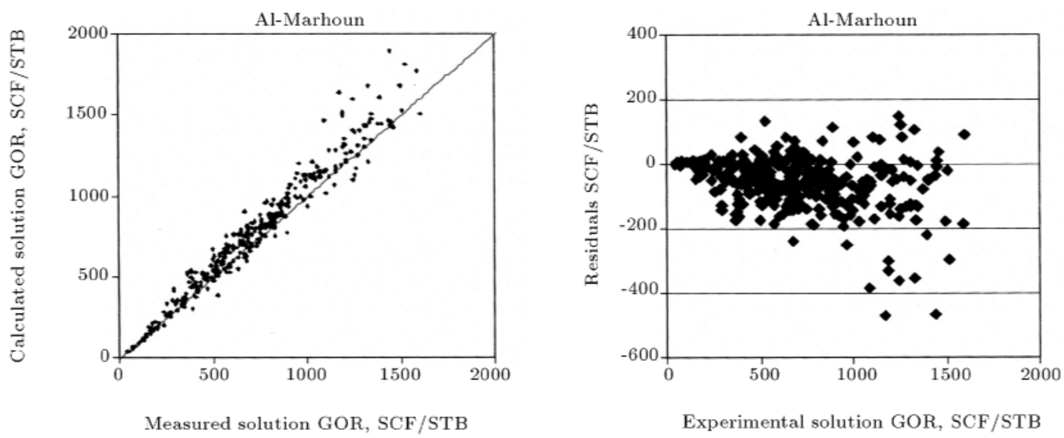

Figure 15. Cross plot and residual plot of R_s (Al-Marhoun [2]) based on Middle East PVT data.

that the Standing [1] and Al-Marhoun [2] correlations have an average absolute deviation of 9.45% and 10.17%, respectively, compared to over 22% for Petrosky. The correlation coefficients are 0.964 and 0.96, respectively, which are close to an ideal value of 1.0. This shows that the Standing and Al-Marhoun correlations correlate better with experimental data than any other correlations.

The maximum error and standard deviation of these correlations are given in Table 5. Figures 15 through 19 give cross plots of the values estimated by the same correlations versus the measured experimental values. It is clear from both Table 5 and Figures 15 through 19 that the Standing and Al-Marhoun correlations are quite superior for Middle East crude oil than other correlations.

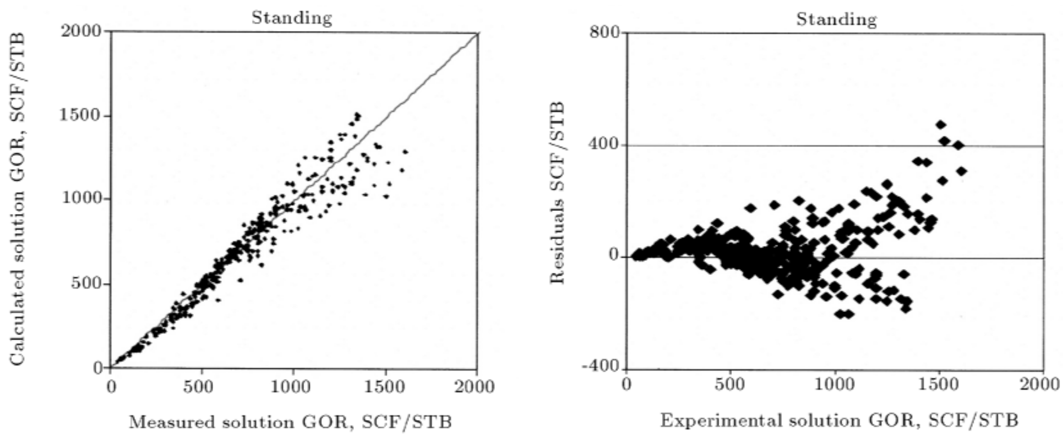

Figure 16. Cross plot and residual plot of R_s (Standing [1]) based on Middle East PVT data.

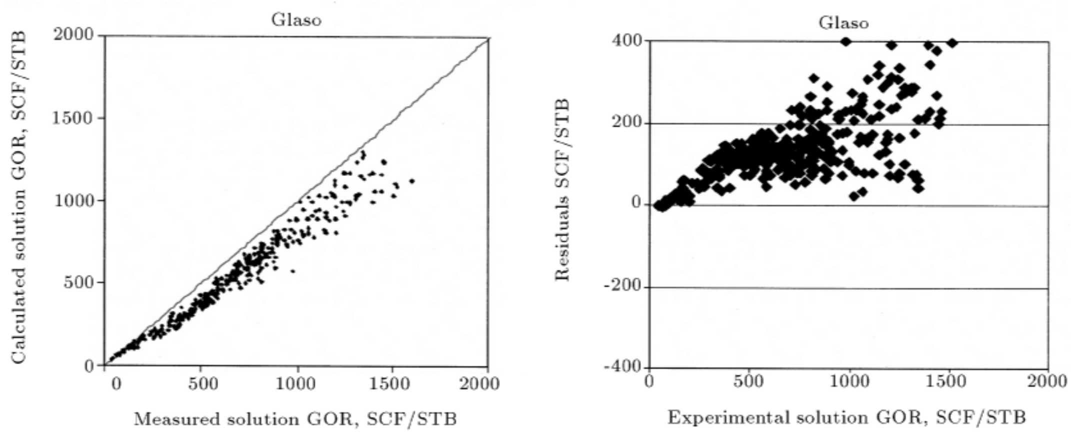

Figure 17. Cross plot and residual plot of R_s (Glaso [3]) based on Middle East PVT data.

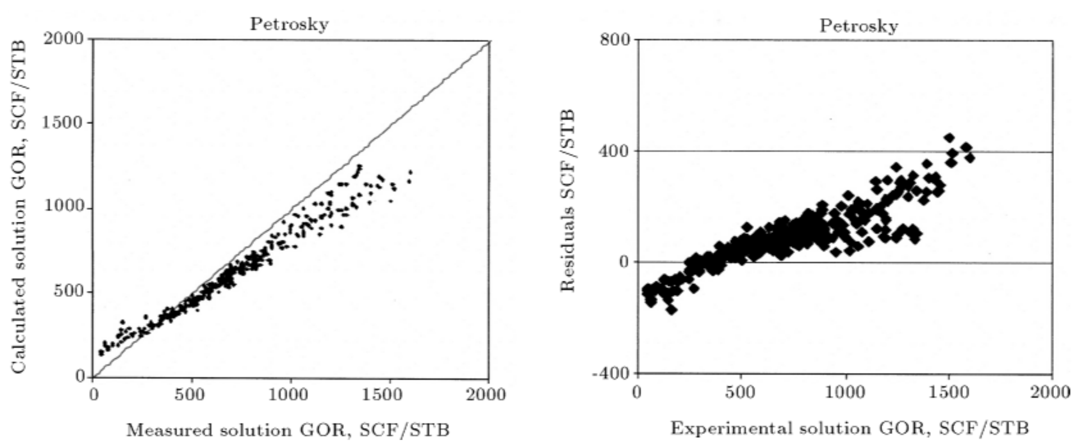

Figure 18. Cross plot and residual plot of R_s (Petrosky [4]) based on Middle East PVT data.

The cross plots of the experimental against the calculated solution GOR using the Standing and Al-Marhoun correlations are presented in Figures 15 and 16. Most of the data points of the new correlation fall very close to the perfect correlation of the 45° line. A graphical plot of residual and experimental solution GOR (shown in Figures 15 and 16) demonstrated a uniform distribution of errors, with most of the data points falling within the ± 200 SCF/STB residual line.

CONCLUSIONS

1. Empirical correlations for Middle East crude oil have been compared for bubble point pressure, the solution gas-oil-ratio, and the bubble point oil formation volume factor;

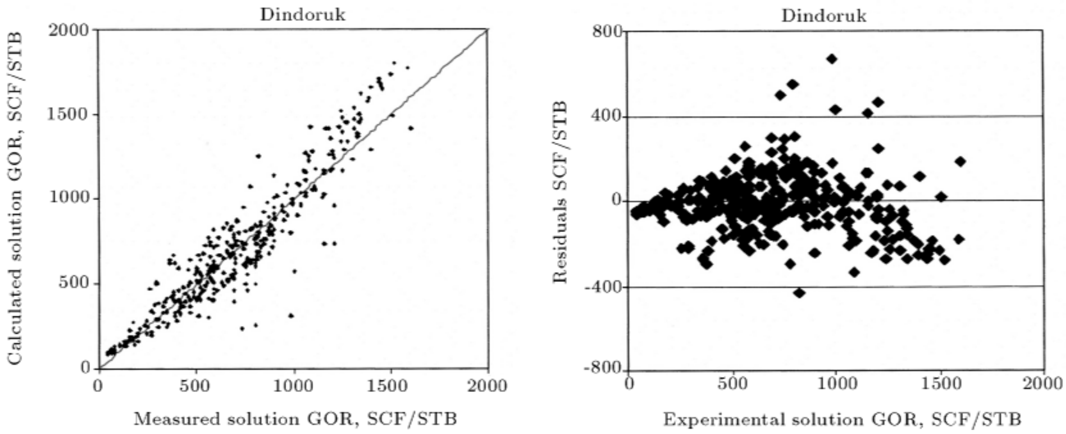

Figure 19. Cross plot and residual plot of R_s (Dindoruk [5]) based on Middle East PVT data.

2. The PVT correlations can be placed in the following order with respect to their accuracy:
   (a) For bubble point pressure, the prediction of Al-Marhoun and Standing are similar to Hanafy and Dindoruk;
   (b) For oil formation volume factor, the results of Petrosky, Glaso, Dokla are near to each other, while Al-Marhoun, Standing and Hanafy correlations are less accurate;
   (c) For solution gas oil ratio, Standing and Al-Marhoun give good results while Dindoruk, Glaso and Petrosky are less accurate.
3. These correlations were compared for Middle East crude oil but they can be used for estimating the same PVT parameters for all types of oil and gas mixture with properties falling within the range of data used in this study;
4. The bubble point oil formation volume factor correlation provided the best accuracy of the correlations evaluated;
5. Correlations are used to generate differential liberation tables for reservoir simulation;
6. Correlations can be tuned for other basins/areas, or for certain classes of oil.

NOMENCLATURE

AAD	absolute average deviation
AAPRE	absolute average percent relative error
API	stock-tank oil gravity, °API
ARE	abosolute relative error
bbl	barrel
B_o	oil formation volume factor, bbl/stb
B_{ob}	oil FVF at bubble point pressure, bbl/stb
Dev.	deviation
FVF	formation volume factor
GOR	gas oil ratio
OFVF	oil formation volume factor
P	pressure, psia
P_b	bubble point pressure, psia
PVT	pressure volume temprature
r	coefficient of correlation
R_s	solution gas-oil-ratio, $\frac{\text{SCF}}{\text{STB}}$
SCF	standard cubic feet
STB	stock tank barrel
Std.	standard
γ_g	gas specific gravity (air = 1)
γ_o	oil specific gravity (water = 1)

Subscripts

b	bubble point
max	maximum
min	minimum
g	gas
o	oil
s	solution

REFERENCES

1. Standing, M.B. "A pressure-volume-temperature correlation for mixtures of California oils and gases", *Drilling and Production Practice*, API, pp 275-287.
2. Al-Marhoun, M.A. "PVT correlations for middle east crude oils", *JPT*, pp 650-665 (1988).
3. Glaso, O. "Generalized pressure-volume-temperature correlations", *JPT*, pp 785-795 (May 1980).
4. Petrosky, G.E. Jr. and Farshad, F.F. "Pressure-volume-temperature correlations for Gulf of Mexico

crude oils", *SPE 26644 Presented at 68th Annual Meeting of the Society of Petroleum Engineers*, Houston, Texas, USA, pp 3-6 (1993).

5. Dindoruk, B., Peter, G. and Christman, "PVT properties and viscosity correlations for Gulf of Mexico oils", *SPE Annual Technical Conference and Exhibition*, New Orleans, Louisiana, 30 September-3 Octobor.
6. Dokla, M. and Osman, M.E. "Correlation of PVT properties for the UAE crudes", *SPE Formation Evaluation*, pp 41-46 (1992).
7. Hanafy, H.H., Macary, S.A., Elnady, Y.M., Bayomi, A.A. and El-Batanoney, M.H. "Empirical PVT correlation applied to Egyptian crude oils exemplify significance of using regional correlations", *SPE 37295, SPE Oilfield Chem. Int. Symp.* (Houston, 2/18-21/97) *Proc.*, pp 733-737 (1997).

APPENDIX

Known PVT Available Correlations for R_s

Standing [1]

$$R_s = \gamma_g \left[\left(\frac{p}{18.2} + 1.4\right) 10^x\right]^{1.2048},$$

$$x = 0.0125\ \mathrm{API} \quad 0.00091(T \quad 460),$$

T = temperature, °R,

p = system pressure, psia,

γ_g = solution gas specific gravity.

Glaso [3]

$$R_s = \gamma_g \left[\left(\frac{\mathrm{API}^{0.989}}{(T \quad 460)^{0.172}}\right)(p_b^*)\right]^{1.2255},$$

$$p_b^* = 10^x,$$

$$x = 2.8869 \quad [14.1811 \quad 3.3093\log(p)]^{0.5}.$$

Al-Marhoun [2]

$$R_s = [a\gamma_g^b \gamma_o^c T^d P]^e,$$

T = temperature, °R,

a = 185.843208,

b = 1.877840,

c = -3.1437,

d = -1.32657,

e = 1.398441.

Petrosky and Farshad [4]

$$R_s = \left[\left(\frac{p}{112.727} + 12.340\right)\gamma_g^{0.8439} 10^x\right]^{1.73184},$$

$$x = 7.916(10 \quad ^4)(\mathrm{API})^{1.5410} \quad 4.561(10 \quad ^5)(T \quad 460)^{1.3911},$$

p = pressure, psia,

T = temperature, °R

Dindoruk and Christman [5]

$$R_{sbp} = \left[\left(\frac{p_{bp}}{a_8} + a_9\right)\gamma_g^{a_{10}} 10^A\right]^{a_{11}},$$

$$A = \frac{a_1 \mathrm{API}^{a_2} + a_3 T^{a_4}}{\left(a_5 + \frac{2API^{a_6}}{p_{bp}^{a_7}}\right)^2}.$$

Coefficient Correlation	Value
a_1	4.86996E-06
a_2	5.7309825539
a_3	9.92510E-03
a_4	1.776179364
a_5	44.25002680
a_6	2.702889206
a_7	0.744335673
a_8	3.359754970
a_9	28.10133245
a_{10}	1.579050160
a_{11}	0.928131344

Known PVT Available Correlations for P_b

Standing [1]

$$p_b = 18.2\left[\left(\frac{R_s}{\gamma_g}\right)^{0.83}(10)^a \quad 1.4\right],$$

$$a = 0.00091(T \quad 460) \quad 0.0125(\mathrm{API}),$$

p_b = bubble-point pressure, psia,

T = system temperature, °R.

Glaso [3]

$$\log(p_b) = 1.7669 + 1.7447\log(p_b^*) \quad 0.30218[\log(p_b^*)]^2,$$

$$p_b^* = \left(\frac{R_s}{\gamma_g}\right)^a (T)^b (\mathrm{API})^c,$$

T = system temperature, °F,

a = 0.816,

b = 0.172,

c =   0.989.

Al-Marhoun [2]

$$p_b = aR_s^b \gamma_g^c \gamma_o^d T^e,$$

T = temperature, °R,

$a = 5.38088 \times 10 \quad ^3,$

$b = 0.715082,$

$c = \;\; 1.87784,$

$d = 3.1437,$

$e = 1.32657.$

Petrosky and Farshad [4]

$$p_b = \left[\frac{112.727R_s^{0.577421}}{\gamma_g^{0.8439}(10)^x}\right] \;\; 1391.051,$$

$$x = 7.916(10^{\;4})(\text{API})^{1.5410}$$

$$\;\; 4.561(10^{\;5})(T \;\; 460)^{1.3911},$$

$p =$ pressure, psia,

$T =$ temperature, °R.

Dokla and Osman [6]

$$p_b = 0.836386$$

$$\times 10^4 \gamma_g^{\;1.01049} \gamma_o^{0.107991} T^{\;0.952584} R_s^{0.724047},$$

$T =$ system temperature, °R.

Dindoruk and Christman [5]

$$p_{bp} = a_8 \left(\frac{R_s^{a_9}}{\gamma_g^{a_{10}}} 10^A + a_{11}\right),$$

$$A = \frac{a_1 T^{a_2} + a_3 \text{API}^{a_4}}{\left(a_5 + \frac{2R_s^{a_6}}{\gamma_g^{a_7}}\right)^2}.$$

Coefficient Correlation	Value
a_1	1.42828E-10
a_2	2.844591797
a_3	-6.74896E-04
a_4	1.225226436
a_5	0.033383304
a_6	-0.272945957
a_7	-0.084226069
a_8	1.869979257
a_9	1.221486524
a_{10}	1.370508349
a_{11}	0.011688308

Known PVT Available Correlations for B_o

Standing [1]

$$B_o = 0.9759 + 0.000120$$

$$\left[R_s\left(\frac{\gamma_g}{\gamma_o}\right)^{0.5} + 1.25(T \;\; 460)\right]^{1.2},$$

$T =$ temperature, °R.

Glaso [3]

$$B_o = 1.0 + 10^A,$$

$$A = \;\; 6.58511 + 2.91329 \log B_{ob}^* \;\; 0.27683(\log B_{ob}^*)^2,$$

$$B_{ob}^* = R_s\left(\frac{\gamma_g}{\gamma_o}\right)^{0.526} + 0.968(T \;\; 460),$$

$T =$ temperature, °R.

Al-Marhoun [2]

$$B_o = 0.497069 + 0.862963 \times 10^{\;3}T + 0.182594$$

$$\times 10^{\;2}F + 0.318099 \times 10^{\;5}F^2,$$

$$F = R_s^a \gamma_g^b \gamma_o^c,$$

$a = 0.742390,$

$b = 0.323294,$

$c = \;\; 1.202040,$

T is the system temperature in °R.

Petrosky and Farshad [4]

$$B_o = 1.0113 + 7.2046(10^{\;5})\Big[R_s^{0.3738}\;\frac{\gamma_g^{0.2914}}{\gamma_o^{0.6265}}\Big)$$

$$+0.24626(T \;\; 460)^{0.5371}\Big]^{3.0936},$$

$T =$ temperature, °R.

Dindoruk and Christman [5]

$$B_{obp} = a_{11} + a_{12}A + a_{13}A^2 + a_{14}(T \;\; 60)\frac{\text{API}}{\gamma_g},$$

$$A = \frac{\left(\frac{R_s^{a_1}\gamma_g^{a_2}}{\gamma_o^{a_3}} + a_4(T \;\; 60)^{a_5} + a_6 R_s\right)^{a_7}}{\left(a_8 + \frac{2R_s^{a_9}}{\gamma_g^{a_{10}}(T \;\; 60)}\right)^2},$$

Coefficient Correlation	Value
a_1	2.510755E+00
a_2	-4.852538E+00
a_3	1.183500E+01
a_4	1.365428E+05
a_5	2.252880E+00
a_6	1.007190E+01
a_7	4.450849E-01
a_8	5.352624E+00
a_9	-6.309052E-01
a_{10}	9.000749E-01
a_{11}	9.871766E-01
a_{12}	7.865146E-04
a_{13}	2.689173E-06
a_{14}	1.100001E-05